Momentum-space method for pionic atoms

A. Cieplý, M. Gmitro,* and R. Mach
Institute of Nuclear Physics, Czechoslovak Academy of Sciences, CS 250 68 Řež, Czechoslovakia

S. S. Kamalov
Laboratory of Theoretical Physics, Joint Institute for Nuclear Research, Dubna, SU 101 000 Moscow, U.S.S.R.
(Received 9 July 1990)

A new momentum-space method is developed for calculation of the strong-interaction shifts and widths in pionic atoms. The singularity connected with the Coulomb potential is treated by using the Vincent and Phatak prescription. The nuclear and atomic distances are separated in our scheme and this secures numerical stability of the calculation. The latter property makes the method a useful alternative to the earlier algorithms. Sample results for a series of light pionic atoms are shown.

I. INTRODUCTION

A momentum-space pion-nuclear optical potential constructed semimicroscopically within the multiple-scattering theory has been shown recently [1] to describe very well the available $\pi^{\pm}$-nucleus ($4 \leq A \leq 40$) elastic and total scattering data for the pion energies $20 \leq T_{\pi} \leq 250$ MeV. The potential contains two phenomenological complex parameters which have been fitted to the available $\pi^{\pm}$-^{12}C data. They turned out to vary smoothly with the energy and are universal with respect to the nuclear mass number A and the pion charge. When compared with the widely used coordinate-space Ericson-Ericson-type pionic atom potentials [2], which are based on the assumption of the zero range of the corresponding πN interaction, the potential of Ref. [1] contains the finite-range features in a natural way.

The goal of the present paper is to develop a momentum-space method for the pionic atoms along the line of Ref. [1]. To illustrate the need for it we mention that, e.g., the coordinate-space formulation of the finite-size (FS) effects [3–5] in the context of the π-mesic atoms leads to the integro-differential equation which can be solved only with a number of additional approximations [5]. The investigation of similar problems of the detailed pion-nuclear dynamics as well as the studies of the respective relativistic features can indeed be simplified if one addresses oneself to the flexible and convenient momentum-space representation [6].

The main difficulty one encounters in studying the atomic systems in the momentum space is the well-known logarithmic singularity associated with the Coulomb potential of point charges which occurs in each pion-nucleus partial wave.

A regularization method had been proposed a few years ago by Kwon and Tabakin [6]. The computer program BOPIT [7], which implements the algorithm by Kwon and Tabakin, is, however, not fully satisfactory since the calculation is rather sensitive to the choice of the integration grid [5–7] which should compromise the requirements dictated by two very different (atomic and nuclear) characteristic scales.

Another regularization procedure for the Coulomb term in the momentum space was developed by Vincent and Phatak [8] in the case of pion-nucleus scattering. In the present paper we show that this formalism can be straightforwardly extended for the solution of the bound pion-nucleus problem. Unlike in the BOPIT program, the integration within the nuclear scale is separated from the integration of the long-range part of the electromagnetic potential and this secures the very stable performance of the algorithm. The idea of the Vincent and Phatak regularization has been mentioned by Kwon and Tabakin [6], but, surprisingly, it has not been exploited in Refs. [6] and [7].

There are a number of interesting physical problems to be solved in order to achieve an understanding of the existing mesoatomic data "anomalous" states, role of the nuclear correlations, and other nuclear structure effects). We plan to consider some of them in the forthcoming articles. In the present paper we limit ourselves to more technical problems. We shall, in Secs. II and III, present the method of mesoatomic calculations based on the Vincent-Phatak algorithm and compare it in Sec. IV with some earlier calculations. Also in Sec. IV, we display some sample calculations of the $1s$ and $2p$ shifts and widths for the light pionic mesoatoms.

II. METHOD

The full pion-nucleus optical potential is taken in the form

$$V = V_C + V_{\rm VP} + V_{\rm FS} + V_N \ , \tag{1}$$

where V_N is the strong-interaction potential and $V_{\rm FS}$ is connected with the electromagnetic corrections due to the extended charge distributions of the nucleus and the pion. The potential V_C corresponds to the Coulomb interaction of the point charges, and finally $V_{\rm VP}$ is the vacuum-polarization potential.

Following Vincent and Phatak [8] we split the potential (1) into the short- and long-distance parts as follows:

$$V=V^{<}+V^{>}\ , \tag{2}$$

$$V^{<}=V\Theta(R-r)\ , \tag{3}$$

$$V^{>}=V\Theta(r-R)\ , \tag{4}$$

where $\Theta(x)=1$ for $x>0$ and $\Theta(x)=0$, otherwise. The matching radius R is taken such that, for $r>R$, it holds with the needed accuracy that

$$(V_{\rm FS}+V_N)\Phi=0\ , \tag{5}$$

where Φ denotes the radial part of the pion-nucleus wave function.

In the outer region ($r>R$) we are then left with the potential

$$V_C(r)+V_{\rm VP}(r)=-\frac{\alpha Z}{r}\left[1+\int_1^{\infty}K(t)e^{-2m_e rt}dt\right]$$
$$=-\frac{\alpha Z}{r}\mathcal{V}(r)\ , \tag{6}$$

where m_e is the electron mass and the function $K(t)$ (to be specified in Sec. III B below) characterizes the vacuum-polarization effects [6,9]. As usual, Z denotes the nuclear charge and α stands for the fine-structure constant.

With the potential (6), we can numerically solve the equation

$$\frac{d^2}{d\rho^2}u_l^{>}(\rho)=\left[\frac{l(l+1)}{\rho^2}+1-\frac{2P}{\rho}\mathcal{V}(r)-\left[\frac{\alpha Z}{\rho}\mathcal{V}(r)\right]^2\delta\right]u_l^{>}(\rho) \tag{7}$$

starting from the asymptotics

$$u_l^{>}(\rho)\xrightarrow[r\to\infty]{}W_{P,\lambda+1/2}(2\rho)\ , \tag{7a}$$

where $W_{P,\lambda+1/2}(2\rho)$ is the well-known Whittaker function [10] and

$$\lambda=[(l+\tfrac{1}{2})^2-(\alpha Z)^2]^{1/2}-\tfrac{1}{2}\quad(\lambda=l)$$

in the relativistic (nonrelativistic) case. Equation (7) with $\delta=0,1$ represents the relativistic Klein-Gordon (KGE, $\delta=1$) or nonrelativistic Schrödinger (SE, $\delta=0$) equation for the lth partial wave. We have denoted $\rho=kr$, where the complex momentum k is related with the total energy $E=E_{nl}-i\frac{1}{2}\Gamma_{nl}$ of the mesoatomic system. The parameter P is proportional to the famous Sommerfeld parameter $P=-i\eta$. The definitions are

$$E=(\mathcal{M}^2-k^2)^{1/2}-\mathcal{M},\quad P=\frac{\alpha Z}{k}(\mathcal{M}^2-k^2)^{1/2} \tag{8a}$$

in the relativistic situation, and

$$E=-\frac{k^2}{2\mathcal{M}},\quad P=\frac{\alpha Z}{k}\mathcal{M} \tag{8b}$$

in the nonrelativistic case. Here $\mathcal{M}$ stands for the pion-nucleus reduced mass.

The solution $u_l^{>}(\rho)$ of Eq. (7) taken at the point $\rho=kR$ will be used in Eq. (10) below for the calculation of the eigenenergy of the system.

The wave function $u_l^{<}(\rho)$, which corresponds to the inner-region potential $V^{<}$, has a plane-wave asymptotics and can be written for $r>R$ as a superposition of the spherical Hankel functions in the form

$$u_l^{<}(\rho)=\rho h_l^{(-)}(i\rho)+[1-2kF_l(k,R)]\rho h_l^{(+)}(i\rho)\ . \tag{9}$$

Matching smoothly at the point $r=R$ the short- and long-range solutions, we obtain the condition

$$\{\rho h_l^{(-)}(i\rho),u_l^{>}(\rho)\}+[1-2kF_l(k,R)]\{\rho h_l^{(+)}(i\rho),u_l^{>}(\rho)\}=0\ , \tag{10}$$

where $\{u,w\}$ denotes the Wronskian $u(dw/d\rho)-(du/d\rho)w$ at the point $\rho=kR$. The discrete complex momenta $k=k_{nl}$ being found as the iterative solutions of Eq. (10), determine the energies and widths of the mesoatomic system.

To solve Eq. (10), we need to know the amplitude $F_l(k,R)$ which fully contains the effects connected with the potential $V^{<}$. Our method of calculating $F_l(k,R)$ goes via the Lippmann-Schwinger (LS) equation solved in the momentum space and we describe it in the next section.

III. AMPLITUDE $F_l(k,R)$

The LS equation for the pion-nucleus scattering matrix $T(E)$ reads as

$$\langle\mathbf{Q}'|T(E)|\mathbf{Q}\rangle=\langle\mathbf{Q}'|U|\mathbf{Q}\rangle+\int\langle\mathbf{Q}'|U|\mathbf{Q}''\rangle G(Q'')\times\langle\mathbf{Q}''|T(E)|\mathbf{Q}\rangle\frac{d^3Q''}{(2\pi)^3}\ , \tag{11}$$

where we defined the Green's function and the potential as

$$G(Q'')=\frac{2\mathcal{M}_\delta}{Q_0^2-Q''^2+i\epsilon},\quad U=V^{<}-\delta\frac{(V^{<})^2}{2\mathcal{M}_\delta}\ . \tag{11a}$$

Here δ has the same meaning as in Eq. (7), $Q_0=ik$ and

$$\mathcal{M}_\delta=\mathcal{M}$$

or

$$\mathcal{M}_\delta=(Q_0^2+\mathcal{M}^2)^{1/2}$$

corresponds to the Schrödinger or Klein-Gordon solution, respectively. Equation (11) can be rewritten in terms of the pion-nucleus partial-wave scattering matrices $T_l(Q',Q,E(Q_0))$ and solved by the matrix-inversion method [11] repeatedly for each (complex) search value E of our eigenvalue iteration process [see Eq. (10)]. The actually needed scattering amplitude $F_l(k,R)$ is then obtained from $T_l(Q_0,Q_0,E(Q_0))$ by the relation

$$F_l(k,R)=-\frac{\mathcal{M}_\delta}{2\pi}T_l(Q_0,Q_0,E(Q_0))\ . \tag{12}$$

The rest of this section is devoted to the construction of

the momentum-space matrix elements of the potential $V^{<}=V\Theta(R-r)$. The quadratic term of the potential U can be treated in the same manner as in Ref. [6].

A. Strong potential

For the strong-interaction part we take the pion-nucleus optical potential as constructed in Ref. [1]. In variance with Ref. [1], we use here the Watson version of the multiple-scattering theory, which allows one a more transparent treatment of Coulomb effects in comparison with the Kerman, McManus, and Thaler formulation.

The semimicroscopic first-order potential is expressed as a product of the isoscalar (a_{00}) and isovector (a_{01}) parts of the scalar pion-nucleon amplitude and the nuclear form factor $F(\mathbf{q})$,

$$\langle \mathbf{Q}'|V_N^{(1)}(E)|\mathbf{Q}\rangle = WA\left[a_{00}+\frac{N-Z}{A}a_{01}\right]F(\mathbf{q}) , \quad \mathbf{q}=\mathbf{Q}'-\mathbf{Q} . \tag{13}$$

The amplitudes a_{00} and a_{01} were constructed from the standard [12] partial πN amplitudes $f^j_{Lt}(q_f,q_i;e)$ with the assumption that the off-shell extrapolation is defined similarly as in the separable-potential model [13], namely,

$$f^j_{Lt}(q_f,q_i;e)=\sigma^j_{Lt}\frac{v^j_{Lt}(q_f)v^j_{Lt}(q_i)}{D^{(+)}_{Ljt}(e)} . \tag{14}$$

Here $\sigma^j_{Lt}=1$ ($\sigma^j_{Lt}=-1$) stands for the repulsive (attractive) πN interaction,

$$\ln[D^{(+)}_{Ljt}(e)]=\frac{1}{\pi}\int_{M+m}^{\infty}\frac{\delta^j_{Lt}(\omega)}{e-\omega}d\omega \tag{15}$$

and $\delta^j_{Lt}(\omega)$ are the pion-nucleon phase shifts. In the actual calculations we always take

$$v^j_{Lt}(q)=v_L(q)=\frac{q^L}{(1+a_0^2q^2)^2} \tag{16}$$

with $a_0^2=0.224$ fm^2.

Note that the angular momentum L (in the π-N c.m. system) differs due to the angle transformation from the momentum l (in the π-nucleus c.m. system). As a matter of fact, every pion-nucleus amplitude F_l receives contributions from all partial amplitudes f^j_{Lt}. For a detailed discussion see Landau [14].

Our separable-potential model defined via Eq. [14] can be put into correspondence with the finite-range model by Kalbermann *et al.* [5]. The zero-range potential of the Ericson-Ericson type, which they start from, is extended in Ref. 5 to the finite range by the form factors $g_L(q_f)$ and $g_L(q_i)$ as

$$f^j_{Lt}(q_f,q_i;e(q_0))=g_L(q_f)f^j_{Lt}(q_0,q_0;e(q_0))g_L(q_i) . \tag{17}$$

Rewriting our Eq. (14) in the form

$$\sigma^j_{Lt}[v^j_{Lt}(q_0)]^2=D^{(+)}_{Ljt}(e(q_0))f^j_{Lt}(q_0,q_0;e(q_0)) , \tag{18}$$

we arrive at the relations

$$g_L(q_f)=\frac{v_L(q_f)}{v_L(q_0)}, \quad g_L(q_i)=\frac{v_L(q_i)}{v_L(q_0)} \tag{19}$$

between the two approaches. While the Gaussian form has been used in Ref. [5] for the functions $g_L(q)$ and the range parameters R_s and R_p have been fitted to the π-mesoatomic data, we take as fixed the parametrization (16) of $v_L(q)$ tested previously [1] in the π-scattering calculations for the low- and medium-energy pions. The range parameter R_p is in Ref. [5] also interpreted in terms of the cutoff mass $\Lambda\sim 1/R_p$. Our parameter $a_0^2=0.224$ fm^2 corresponds to $\Lambda=0.42$ GeV, a value much smaller than those shown in Table 2 of Ref. [5]. It seems, however, that the pionic atoms do not provide any sensitive ground to test this parameter [5].

The factor

$$W=-2\pi[\mu(Q',p')\mu(Q,p)]^{-1/2} , \tag{20}$$

which appears in Eq. (13), takes into account the relativistic relation between the t matrix and the pion-nucleon amplitude [15]. We define

$$\mu(Q,p)=E_\pi(Q)E_N(p)/\omega(q_i) \tag{21}$$

and

$$\omega(q_i)=\{[E_\pi(Q)+E_N(p)]^2-(\mathbf{Q}+\mathbf{p})^2\}^{1/2} , \tag{22}$$

where the pion energy

$$E_\pi(Q)=(m^2+Q^2)^{1/2}$$

and the total nucleon energy

$$E_N(p)=(M^2+p^2)^{1/2}$$

is evaluated for the effective nucleon moment

$$\mathbf{p}\longrightarrow\mathbf{p}_{\text{eff}}=-\frac{\mathbf{Q}}{A}+\frac{A-1}{2A}(\mathbf{Q}'-\mathbf{Q}) . \tag{23}$$

Using the "factorization" approximation [16] one avoids, without any serious loss of accuracy, the numerical averaging of the nucleonic Fermi motion normally needed in Eq. (13). Expressions analogous to Eqs. (21)–(23) also hold for $\mu(Q',p')$, $\omega(q_f)$, and $\mathbf{p}'_{\text{eff}}$, respectively.

The relative pion-nucleon momenta $\mathbf{q}_f$ and $\mathbf{q}_i$ are given in terms of the pion-nucleus momenta $\mathbf{Q}'$ and $\mathbf{Q}$ by the approximate relativistic formulas

$$\mathbf{q}_f=\mu(Q',p')\left[\frac{\mathbf{Q}'}{E_\pi(Q')}-\frac{\mathbf{p}'}{E_N(p')}\right] , \quad \mathbf{q}_i=\mu(Q,p)\left[\frac{\mathbf{Q}}{E_\pi(Q)}-\frac{\mathbf{p}}{E_N(p)}\right] , \tag{24}$$

the accuracy of which was discussed earlier [15]. The energy dependence

$$e=E-\left\{(m+M)^2+\left[\frac{A-1}{2A}(\mathbf{Q}'+\mathbf{Q})\right]^2\right\}^{1/2} -\left\{(M_A-M)^2+\left[\frac{A-1}{2A}(\mathbf{Q}'+\mathbf{Q})\right]^2\right\}^{1/2}+m+M \tag{25}$$

with M_A for the nuclear mass appears to be a natural relativistic expression obtained in the Galileo-invariant $(A+1)$-body optical model [16,17].

The first-order potential $V_N^{(1)}(E)$ just described has been phenomenologically extended in Ref. [1]. Here we follow the same line. The full strong-interaction potential adopted by us is

$$V_N(E)=V_N^{(1)}(E)+V_N^{(2)}(E) ,$$

where

$$\langle \mathbf{Q}'|V_N^{(2)}(E)|\mathbf{Q}\rangle=-\frac{2\pi}{\mathcal{M}}A(A-1)\left[dB_0+\frac{C_0}{d}\mathbf{Q}'\cdot\mathbf{Q}\right]\times\frac{v_0(Q')v_0(Q)}{[v_0(Q_0)]^2}G(\mathbf{q}) \quad (26)$$

depends on the Fourier transform $G(\mathbf{q})$ of the nuclear density squared $\rho^2(r)$, and $d=1+\frac{1}{2}m/M$, where m (M) is the pion (nucleon) mass. In Eq. (26) we use the form factors $v_0(q)$ of Eq. (16) to define the off-shell extrapolation. Note that the Lorentz-Lorenz renormalization and spin effects are not considered in our potential $V_N^{(1)}(E)+V_N^{(2)}(E)$.

As it was already mentioned in the Introduction, the parameters B_0 and C_0, when fitted to the scattering data in Ref. 1, appeared to be A independent for the nuclei with $A\leq 40$. Such a success of the potential $V_N^{(1)}(E)+V_N^{(2)}(E)$, as defined by Eqs. (13) and (26) in the scattering calculations, has actually motivated the present application to the mesoatomic problems.

B. Coulomb interaction and the electromagnetic corrections

The just calculated matrix $\langle \mathbf{Q}'|V_N(E)|\mathbf{Q}\rangle$ of the strong potential should be supplemented with the electromagnetic terms of $V^<$ as follows: The Coulomb potential in the inner region $(r<R)$ has the Fourier transform

$$\langle \mathbf{Q}'|V_C\Theta(R-r)|\mathbf{Q}\rangle=-2\pi Z\alpha R^2\left[\frac{\sin(\frac{1}{2}qR)}{\frac{1}{2}qR}\right]^2 , \quad (27)$$

which is free from the singularity discussed in the Introduction.

The Fourier transform of the vacuum-polarization term $V_{\rm VP}\Theta(R-r)$ is expressed (see, for comparison, Eqs. (25)–(28) of Ref. [7]) as

$$\langle \mathbf{Q}'|V_{\rm VP}\Theta(R-r)|\mathbf{Q}\rangle=-4\pi Z\alpha R^2F_\pi(q)F_N(q)F(q)\int_1^\infty dt\frac{K(t)}{x^2+y^2t^2}\left[1-e^{-yt}\cos x-\frac{yt}{x}e^{-yt}\sin x\right] , \quad (28)$$

where $x=qR$ and $y=m_eR$. The function $K(t)$ has been taken in the form of the Uehling formula [7,9]

$$K(t)=\frac{2\alpha}{3\pi}\left[1+\frac{1}{2t^2}\right]\frac{(t^2-1)^{1/2}}{t^2}+K_4(t) , \quad (29)$$

where we have corrected errors having appeared in Refs. [6] and [7]. Here the first term is connected with the effects of the order $\alpha Z\alpha$ and the lengthy expression for $K_4(t)$ corresponding to the corrections of the order $\alpha^2Z\alpha$ can be found in Ref. [7].

The corrections due to the finite distributions of the nuclear and pionic charges assume the form

$$\langle \mathbf{Q}'|V_{\rm FS}|\mathbf{Q}\rangle=-4\pi\frac{\alpha Z}{q^2}[F_\pi(q)F_N(q)F(q)-1] . \quad (30)$$

In Eqs. (28) and (30) above, the pionic $[F_\pi(q)]$ and nucleonic $[F_N(q)]$ form factors are taken as equal, namely,

$$F_\pi(q)=F_N(q)=\left[1+\frac{q^2}{0.71\ \text{GeV}^2}\right]^{-2} . \quad (31)$$

The nuclear form factor $F(q)$ describes the distribution of the nucleonic centers within the nucleus and is connected with the observed charge form factor $F_{\rm ch}(q)$ as

$$F_{\rm ch}(q)=F_N(q)F(q) .$$

For the complete specification of the optical potential $V_N(E)$, we also need the Fourier transform of the nuclear density squared

$$G(\mathbf{q})=\int e^{i\mathbf{q}\cdot\mathbf{r}}\rho^2(r)d^3r . \quad (32)$$

In the actual calculation we have extensively used the three-parametric Fermi density [18] $(3pF)$, the harmonic-oscillator density [18] (HO), and the symmetrized Fermi density [1] (SF). It is apparently well known to the practitioners that the mesoatomic characteristics depend only slightly on the functional form of $\rho(r)$: Two densities, $\rho_1(r)$ and $\rho_2(r)$, provide practically equal π-atomic shifts (both of electromagnetic origin and those due to the strong interaction) and widths if they are fitted to the same magnitude of the nuclear charge radius.

Specifically, the numerical results shown below were calculated for ^{3}He, ^{7}Li, ^{9}Be, ^{10}B, and ^{11}B with the harmonic-oscillator form factor

$$F(q)=\left[1-\frac{A-4}{6A}a^2q^2\right]e^{-a^2q^2/4} \quad (33)$$

(omitting the second term in the parenthesis for ^{3}He) and the corresponding expression for $G(q)$. The adopted values of the parameter a are displayed in Table I.

The rest of our examples have been calculated with the symmetrized Fermi density distribution [1,19]

$$\rho(r)=\rho_0\frac{\sinh(c/b)}{\cosh(c/b)+\cosh(r/b)} . \quad (34)$$

Analytical expressions for $F(q)$ and $G(q)$ are given in Ref. 1. The parameters b and c are displayed in Table II.

TABLE I. Parameters of the harmonic-oscillator density distribution $\rho_{HO}(r)$. The values of $a^2=2A(R_{ch}^2-r_p^2)/(5A-8)$ were taken from Ref. [18].

Nucleus	^{3}He	^{7}Li	^{9}Be	^{10}B	^{11}B
a (fm)	1.385	1.619	1.663	1.595	1.560
R_{ch} (fm)	1.88	2.39	2.519	2.45	2.42

They were taken from Refs. [1] and [19] and partly obtained as our own fit.

IV. THE NUMERICAL PERFORMANCE AND COMPARISON WITH OTHER COMPUTATIONS

Equation (10) has been solved by the simplex method. In the test calculation for the pure point-Coulomb potential ($V_N+V_{VP}+V_{FS}=0$), we were able to reproduce the Bohr energies of the $1s$ and $2p$ orbits with relative accuracy always better than 10^{-5} in the nonrelativistic and relativistic cases. For a comparison we have performed analogous calculations with the code BOPIT [7]. With the grid parameters recommended in Ref. [6] BOPIT leads to a precision roughly equal to 10^{-4} in both of the above cases, e.g., for $1s$ level in the ^{16}O mesoatom. As one can see from Table III, varying the number of grid points from 48 to 16, the precision of our method remains practically the same. Actually, only about 20 grid points are needed for obtaining very stable and precise results. Our experience tells us that the high numerical accuracy of the present method is preserved even if the other parts of the pion-nucleus potential (V_{FS}, V_{VP}, V_N) are included. This is because the atomic ($r>R$) and nuclear ($r<R$) domains are treated separately in the coordinate and momentum space, respectively. Unlike the Kwon-Tabakin approach [6], where the choice of the grid point distribution requires a special attention, our solutions turn out to be very stable under variations in a number of mesh points and in their distribution. With this development we now have a practical alternative to the BOPIT [7] program. The present algorithm is certainly superior to the predecessor in much higher numerical stability. To obtain accurate results, one should only choose the matching parameter R as small as possible: $R=7-10$ fm is a reasonable choice complying with condition (5).

All further calculations were performed by solving the Schrödinger equation inserting, however, the optical potential which contains the relativistic corrections described in Sec. III A. We proceed so as to avoid possible problems arising in the relativistic case due to the ambiguity of introducing the strong-interaction potential into the Klein-Gordon equation.

In the second series of our tests we have calculated the energy shifts due to the nuclear finite-size and the vacuum-polarization corrections. The latter are calculated to the order $\alpha^2 Z\alpha$ and also include the effects of the nuclear size. All the results presented in Table IV were obtained for the point charge of an orbiting pion. Comparing the energy shifts ΔE_{FS} obtained in Refs. [6] and [20] shown in Table IV, one can see that they differ by about 10% (20%) for the FS shifts of the $1s$ ($2p$) levels. To trace the origin of such differences is, however, very difficult since this is a result of different approximations adopted in calculations but insufficiently specified by various authors. In particular, the calculated values of ΔE_{FS}, although fully insensitive to the functional form adopted for the nuclear density distribution $\rho(r)$, depend strongly on the value of the nuclear charge radius R_{ch} corresponding to the chosen distribution $\rho(r)$. The experimental values of R_{ch} may differ by a few percent, this leads to a 10–15% change of the calculated ΔE_{FS}. Our theoretical values of ΔE_{FS} lie mostly between those obtained by BOPIT and the ones quoted in Ref. [20].

As for the calculated vacuum-polarization corrections ΔE_{VP} shown in Table IV, we note that our results are rather close to those obtained with the BOPIT code [7]. At the same time, the values of ΔE_{VP} collected in the re-

TABLE II. Parameters of the symmetrized Fermi density distribution. Note that $R_{ch}^2=\frac{1}{5}[7(\pi b)^2+3c^2]+r_p^2$, where we take $r_p=0.81$ fm.

Nucleus	b (fm)	c (fm)	R_{ch} (fm)
^{4}He	0.300	1.251	1.685
^{6}Li	0.566	1.342	2.483
^{12}C	0.393	2.275	2.428
^{13}C	0.356	2.315	2.372
^{14}N	0.393	2.450	2.529
^{16}O	0.404	2.624	2.654
^{19}F	0.507	2.629	2.891
^{20}Ne	0.502	2.771	2.958
^{23}Na	0.498	2.875	3.007
^{24}Mg	0.484	2.984	3.039
^{28}Si	0.477	3.134	3.114
^{32}S	0.520	3.291	3.300
^{40}Ca	0.493	3.593	3.430
^{56}Fe	0.490	4.156	3.787

TABLE III. The relative accuracy $|(E-E_B)/E_B|$ achieved in reproducing the Bohr energy E_B in the case of $1s$ level in pionic ^{16}O. The results obtained using our code PIATOM and BOPIT [7] in the relativistic (KGE) and nonrelativistic (SE) cases are compared for different number of grid points (NP).

NP	BOPIT		PIATOM	
	KGE	SE	KGE	SE
48	5.4×10^{-5}	5.5×10^{-5}	4.0×10^{-6}	3.0×10^{-6}
40	6.6×10^{-5}	7.1×10^{-5}	6.3×10^{-6}	5.2×10^{-6}
32	1.1×10^{-4}	1.1×10^{-4}	9.6×10^{-6}	8.5×10^{-6}
24	2.8×10^{-4}	2.9×10^{-4}	5.1×10^{-5}	3.8×10^{-5}
16	6.9×10^{-4}	7.0×10^{-4}	8.4×10^{-5}	6.4×10^{-5}

TABLE IV. The energy shifts due to the nuclear finite-size (ΔE_{FS}) and vacuum-polarization effects (ΔE_{VP}) for several π-atomic levels. Our results are presented in comparison with the values obtained previously by using the momentum [6] and coordinate [20] space techniques. The notation of charge distribution used is the following: (a) harmonic oscillator for 1s-level calculation and two-parameter Fermi density for 2p-level calculations, (b) nuclear density not specified in Ref. [20] and (c) symmetrized Fermi density.

		ΔE_{FS} (eV)			$-\Delta E_{VP}$ (eV)		
Nucleus	Level	Ref. [6] (a)	Ref. [20] (b)	Present (c)	Ref. [6] (a)	Ref. [20] (b)	Present (c)
^{12}C	1s	897	810	848	642	540	624
^{14}N	1s	1744	1570	1661	954	750	917
^{16}O	1s	3266	3160	3029	1278	980	1271
^{32}S	2p	27	20	25	777	660	801
^{40}Ca	2p	119	100	100	1352	1150	1460

view article by Backenstoss [20] are systematically lower roughly by 20%. This is due to different approximations adopted for ΔE_{VP} in Ref. [20]. In particular, those calculations are performed to the order $\alpha Z\alpha$ and neglect the nuclear finite-size effects.

One can summarize that our results for the energy shifts connected with the electromagnetic effects are stable and consistent with analogous evaluations.

A. Illustrative examples of the strong-interaction shifts and widths

Here we shall display several examples of the calculated mesoatomic level shifts ΔE_N and the absorption widths Γ_{ABS} defined as

$$E(nl)=E_B(nl)+\Delta E_{EM}(nl)+\Delta E_N(nl)-\frac{i}{2}\Gamma_{ABS}(nl) \ . \quad (35)$$

Here, E_B are energies of the Bohr orbits and ΔE_{EM} represents the summed contribution due to the finite distributions of the nuclear and pionic charges and the vacuum-polarization corrections.

The calculations were performed for the 1s and 2p levels of the light ($A \leq 56$) pionic mesoatoms. To fix the parameters B_0 and C_0 of the optical potential (26), we have used the most accurate, available, 1s-level data for the pionic ^{12}C [21,22] and ^{16}O [23] and for the 2p-level data of pionic ^{32}S and ^{40}Ca [24]. The result of the fit is

$$B_0=(-0.093+i0.042)m^{-4} \ ,$$

$$C_0=(-0.125+i0.090)m^{-6} \ .$$

These values have been used in all the calculations to be discussed below.

Before comparing our calculations with the results of previous studies, one should notice that the (small) isoscalar combination of the πN s-wave partial amplitudes (usually denoted as b_0) has been kept fixed in our fitting procedure as it corresponds to its microscopic origin in Eq. (13). Further, the second-order Pauli correction sometimes added to b_0 as, e.g., in Ref. [2], is expected to be absorbed into the coefficient B_0. Since there is a strong correlation between the values of b_0 and $\mathrm{Re}B_0$, we have obtained a larger negative value for $\mathrm{Re}B_0$ corresponding to a strong s-wave repulsion. The value of $\mathrm{Im}B_0$ was obtained in an agreement with the results of other analyses [25]. As for the numerical value of C_0, it always depends on the particular form of the optical potential taken by different authors. Our values of $\mathrm{Re}C_0$ and $\mathrm{Im}C_0$ lie within the boundaries found in earlier works. The negative sign of the ratio $\mathrm{Re}C_0/\mathrm{Im}C_0=-1.4$ is in agreement with the neglect of the Lorentz-Lorenz anticorrelations in Eqs. (13) and (26) (see also, Ref. [26]).

Our results for the 1s levels are shown in Fig. 1. The calculated values of $\Gamma_{ABS}(1s)$ for 15 mesoatoms are connected by a full line in Fig. 1(b) and compared with the data. In Fig. 1(a) the full line visualizes the nuclear shifts $\Delta E_N(1s)$ for the $T_Z=0$ nuclei and the dashed line those for the $T_Z=\frac{1}{2}$ nuclei. The energy shift for the ^{3}He pionic mesoatom ($T_Z=-\frac{1}{2}$) is actually of an opposite sign and we present it in this way to simplify the picture. Our result is indicated by a star at the corresponding point. As one can see, the well-known isospin dependence of ΔE_N is very well reproduced in Fig. 1(a). The most serious discrepancy between the calculated and measured data is in the case of ^{4}He; this was also observed in the earlier coordinate-space calculations [27,22]. We have performed a separate fit of the parameter B_0 for ^{4}He with the results

$$B_0=(-0.063+i0.028)m^{-4} \ ,$$

C_0 being the same as above. To improve the agreement of the calculated shifts and widths for mesoatoms of $A \leq 16$ nuclei, one should replace the ρ^2 term by a more realistic two-nucleon correlation function. We expect the long-range recoil correlations to strongly influence the calculated characteristics of the lightest mesoatoms. The corresponding calculations are in progress.

The characteristics of the 2p level are shown in Fig. 2. The measured 2p-level widths are very well reproduced in the whole interval $12 \leq A \leq 56$. The agreement between the calculated and experimental strong shifts $\Delta E_N(2p)$ is worse; in particular, the precise measurements for the ^{24}Mg and ^{28}Si do not follow the trend of the other data. Apparently, more details of the nuclear structure might be needed in the construction of the optical potential for

these open-shell nuclei. For instance, the $\sigma \cdot l$ term obtained by Mach [28] in the context of the pion-nucleus scattering and discussed some time ago by Friedman and Gal [26] for the pionic atoms could be of importance here.

Our calculated absorption widths are closer to the data than in the case for the strong energy shifts if the comparison with experiment is performed in a straightforward fashion. As a matter of fact, the measurements of the transmission energies in the pionic atoms are really very precise. The evaluated experimental magnitudes of the shifts ΔE_N contain, however, some systematic errors connected with the calculations of the electromagnetic corrections. Due to them (see Table IV and the discussion in Sec. IV), one should admit that the published experimental errors are unrealistically diminished. It seems [29] that an error of no less than 5% should be expected for the measured ΔE_N. This indeed means that the data presented in Figs. 1(a) and 2(a) may bear error bars much larger than the published ones.

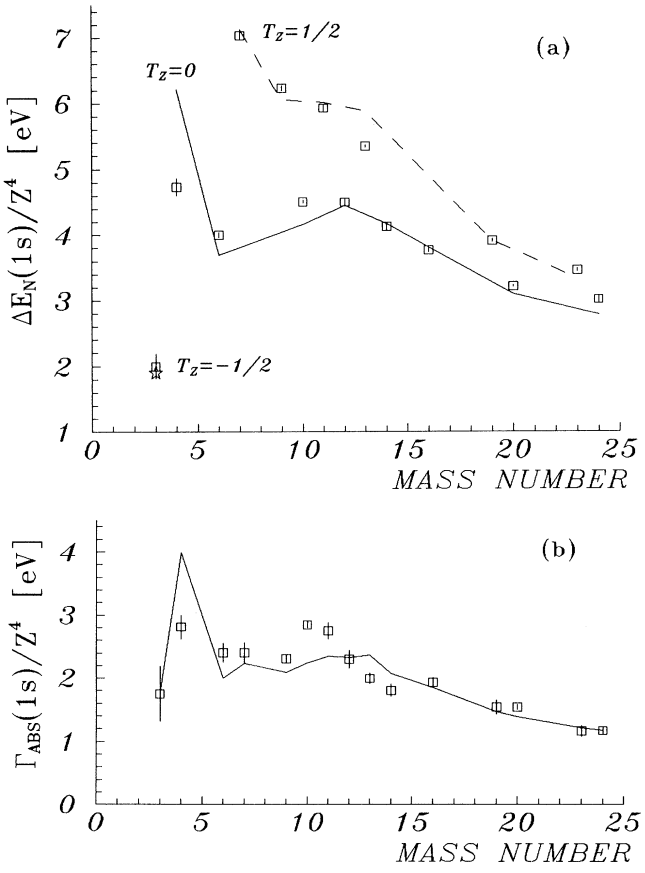

FIG. 1. Comparison of the 1s-level calculated pionic atom energy shifts ΔE_N (a) and widths Γ_{ABS} (b) with the data. A star denotes the ^{3}He ($T_Z=-\frac{1}{2}$) calculated result, the full (dashed) line connects the theoretical values for the $T_Z=0$ ($T_Z=\frac{1}{2}$) nuclei. Data are from Ref. [21] (^{12,13}C), Ref. [22] (^{4}He, ^{6,7}Li, ^{9}Be, ^{12}C, ^{14}N), Ref. [23] (^{3}He, ^{16}O), Ref. [30] (^{10,11}B), Ref. [31] (^{19}F), Ref. [32] (^{20}Ne), Ref. [33] (^{23}Na), and Ref. [34] (^{24}Mg).

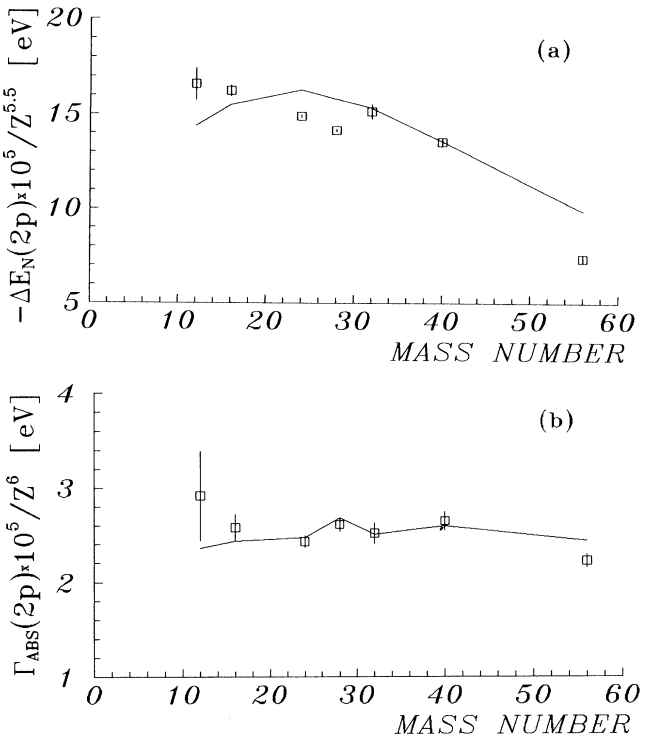

FIG. 2. The same as Fig. 1 but for the 2p-level shifts and widths. Data are from Ref. [35] (^{12}C, ^{16}O, ^{24}Mg, ^{28}Si) and Ref. [24] (^{32}S, ^{40}Ca, ^{56}Fe).

Systematic calculations of the shifts and widths of the light mesoatoms are not numerous in the literature. In the present, rather technical, paper we refrain from the comparisons which would concern the details of the physics studied by various authors. In general, the agreement of the calculated shifts and widths with the data might be remarkably better than ours [25,27]. In this connection it is appropriate to comment that usually six to seven free parameters of the pionic potential are fitted so as to bring the calculated mesoatomic characteristics as close as possible to the experimental values. At the same time, the potential V_N used in the present calculations contains only four free parameters.

V. SUMMARY

We have, in detail, presented a different momentum-space method for the calculations of the strong shifts and widths of the pionic mesoatoms. The method is very satisfactory in the numerical performance. The precision of results is remarkably higher in comparison with that obtained by using other computer codes. The new algorithm is practically insensitive in a broad interval to the choice of integration grid.

Our optical potential is constructed in the momentum space and therefore retains the important effects connected with the 2-c.m. $\rightarrow$ A-c.m. frame transformation including the so-called angle transformation. Simultaneously, it provides the technical means for an appropriate consideration of the nucleonic Fermi motion and nonlocality

of the πN amplitude (within the separable-potential model). An A universal quartet of phenomenological parameters of the optical potential has been shown to provide an adequate description of the mesoatomic characteristics in the interval $A \leq 56$ which we have investigated.

Although it has not been our goal in this article to study the physics of the pionic mesoatoms, we show, as a demonstration, a rather extensive sample of the $1s$- and $2p$-level characteristics and compare them with the data. That comparison should only illustrate the calculation feasibility of the method. In our opinion, the individuality of the light nuclei is too rich to try a quantitative description of the corresponding mesoatomic characteristics in terms of $\rho(r)$ and $\rho^2(r)$ exclusively. We expect that consideration of the nuclear correlations, spin-dependent terms, and spin-orbital terms for the non-closed-shell nuclei is obligatory for a reliable analysis of the light pionic mesoatoms. The suggested method is well suited for this work. The results will be reported elsewhere.

Noted added in proof. We have performed also the relativistic calculations solving the corresponding KGE. Using the same charge distributions as in [6] we returned with practically the same results as those presented in Table IV, columns (a) provided that the authors of [6] calculated their values of $\Delta E_{\rm VP}$ including also the corrections due to FS of pion. Further in the case of $2p$ level they probably do not present the shifts $\Delta E_{\rm VP}$ but the summed value $\Delta E_{\rm EM}$.

---

*Deceased, October 10, 1990.

[1] M. Gmitro, S. S. Kamalov, and R. Mach, Phys. Rev. C **36**, 1105 (1987).

[2] M. Ericson and T. E. O. Ericson, Ann. Phys. (N.Y.) **36**, 323 (1966).

[3] K. L. Giovanetti, G. De Chambrier, P. F. A. Goudsmit, H. J. Leisi, B. Jeckelmann, and Th. Karapiperis, Phys. Lett. B **186**, 9 (1987).

[4] E. Friedman, A. Gal, G. Kalbermann, and C. J. Batty, Phys. Lett. B **200**, 251 (1988).

[5] G. Kalbermann, E. Friedman, A. Gal, and C. J. Batty, Nucl. Phys. **A503**, 632 (1989).

[6] Yong Rae Kwon and F. Tabakin, Phys. Rev. C **18**, 932 (1978).

[7] D. P. Heddle, Yong Rae Kwon, and F. Tabakin, Comput. Phys. Commun. **38**, 71 (1985).

[8] C. M. Vincent and S. C. Phatak, Phys. Rev. C **10**, 391 (1974).

[9] E. A. Uehlig, Phys. Rev. **48**, 55 (1935).

[10] I. J. Thompson and A. R. Barnett, Comput. Phys. Commun. **36**, 363 (1985).

[11] M. Gmitro, J. Kvasil, and R. Mach, Phys. Rev. C **31**, 1349 (1985).

[12] J. M. Eisenberg and D. Koltun, *Theory of Meson Interations with Nuclei* (Wiley, New York, 1980).

[13] T. Londergan, K. M. McVoy, and E. J. Moniz, Ann. Phys. (N.Y.) **86**, 147 (1974).

[14] R. H. Landau, S. C. Phatak, and F. Tabakin, Ann. Phys. (N.Y.) **78**, 299 (1973).

[15] R. Mach, Nucl. Phys. **A205**, 56 (1973).

[16] R. H. Landau and A. W. Thomas, Nucl. Phys. **A302**, 461 (1978).

[17] R. Mach, Czech. J. Phys. B **33**, 549 (1983); **33**, 616 (1983); **33**, 772 (1983).

[18] C. W. De Jager, H. De Vries, and C. De Vries, At. Data Nucl. Data Tables **14**, 479 (1974); **36**, 495 (1987).

[19] V. V. Burov and V. K. Lukyanov, Joint Institute for Nuclear Research, Dubna Report P4-11098, 1977.

[20] G. Backenstoss, Annu. Rev. Nucl. Sci. **20**, 467 (1970).

[21] C. A. Fry, G. A. Beer, G. R. Mason, R. M. Pearce, P. R. Poffenberger, C. I. Sayre, A. Olin, and J. A. Macdonald, Nucl. Phys. **A375**, 325 (1982).

[22] L. Tauscher and W. Schneider, Z. Phys. **271**, 409 (1974).

[23] I. Schwanner, G. Backenstoss, W. Kowald, L. Tauscher, H.-J. Weyer, D. Gotta, and H. Ullrich, Nucl. Phys. **A412**, 253 (1984).

[24] C. J. Batty, S. F. Biagi, E. Friedman, S. D. Hoath, J. D. Davies, G. J. Pyle, G. T. A. Squier, D. M. Asbury, and A. Guberman, Nucl. Phys. **A322**, 445 (1979).

[25] C. J. Batty, Fiz. Elem. Chastits At. Yadra **13**, 164 (1982) [Sov. J. Part. Nucl. **13**, 71 (1982)].

[26] E. Friedman and A. Gal, Nucl. Phys. **A345**, 457 (1980).

[27] C. J. Batty, E. Friedman, and A. Gal, Nucl. Phys. **A402**, 411 (1983).

[28] R. Mach, Nucl. Phys. **A258**, 513 (1976).

[29] J. Nieves, E. Oset, and C. Garcia-Recio, University Valencia Report FTUV/89-30, 1989.

[30] A. Olin, P. R. Poffenberger, G. A. Beer, J. A. Macdonald, G. R. Mason, R. M. Pearce, and W. C. Sperry, Nucl. Phys. **A360**, 426 (1981).

[31] A. Olin, G. A. Beer, D. A. Bryman, M. S. Dixit, J. A. Macdonald, G. R. Mason, R. M. Pearce, and P. R. Poffenberger, Nucl. Phys. **A312**, 361 (1978).

[32] B. H. Olaniyi, G. A. Beer, A. Fry, J. A. Macdonald, G. R. Mason, A. Olin, R. M. Pearce, and P. R. Poffenberger, Nucl. Phys. **A384**, 345 (1982).

[33] D. I. Britton, G. A. Beer, J. A. Macdonald, G. R. Mason, T. Numao, A. Olin, P. R. Poffenberger, A. R. Kunselman, and B. H. Olaniyi, Nucl. Phys. **A461**, 571 (1987).

[34] A. Taal, Ph.D. thesis, National Instituut voor Kernfysica en Hoge-Energiefysica, 1988.

[35] G. De Chambrier *et al.*, Nucl. Phys. **A442**, 637 (1985).